Detailed Study of Potassium Solvation Using Molecular Dynamics Techniques

Tsun-Mei Chang and Liem X. Dang*

Environmental Molecular Sciences Laboratory, Pacific Northwest National Laboratory, Richland, Washington 99352

Received: May 1, 1998; In Final Form: April 1, 1999

Molecular dynamics simulations are carried out to examine the solvation properties and the ion-solvation shell exchange process of the K^+ ion in liquid water, chloroform, and carbon tetrachloride. The solvent molecules are found to form well-defined solvation shells around the K^+ ion and show a preferred orientational order toward the ion. The induced dipole moment distribution of K^+ becomes broader and shifts to a larger average value from chloroform to carbon tetrachloride to water. It is observed that the K^+ ion diffuses more rapidly in the aqueous phase than in liquid chloroform and carbon tetrachloride. We have also evaluated both ion and first solvent shell velocity autocorrelation functions and the residence time autocorrelation functions for the ion in water, chloroform, and carbon tetrachloride. The residence time is found to be 9.4 ps for water and about 30 ps for both chloroform and carbon tetrachloride. By use of a constrained molecular dynamics technique, the first solvation shell exchange process is investigated. It is found that an estimate using equilibrium solvation and classical transition-state theory overestimates the dissociation rate of the K^+ ion. Including the dynamical effects using Grote−Hynes theory yields more accurate dissociation rates.

I. Introduction

In the past, a considerable theoretical and computational effort has been devoted to the understanding of the solvation of ions and solutes in aqueous solutions.[1−8] The study of ion solvation in organic and inorganic liquids has received some attention because of the fact that nonaqueous solvents play an important role in chemistry.[9−11] The motivation for the present work is to characterize the ionic solvation in various solvents (i.e., water, chloroform, and carbon tetrachloride) and to correlate the observed solvation properties with the nature of the solvents. Because of the strong electric field induced by the ion in the ion−solvent systems, an explicit treatment of the molecular polarizability for both solute and solvent molecules will provide a more realistic description of the structural and solvation properties of the K^+ ion in various solvents.

In the present paper, we carry out molecular dynamics simulations to examine the solvation properties of K^+ ion liquid water and chlorinated hydrocarbons (chloroform and carbon tetrachloride). The interest in studying ion solvation processes in chlorinated hydrocarbons is of particular importance to environmental remediation. It is well-known that chloroform and carbon tetrachloride are widely used in laboratories and throughout industry. In addition, chloroform and carbon tetrachloride are utilized as a solvent in the processing of radioactive materials and thus contributes significantly to the nuclear waste problems.[12] A detailed investigation of the solvation properties and the molecular interactions between the ions and the chlorinated hydrocarbons will further the understanding of these environmental issues. Our ultimate goal is to study the transport properties of ions across these liquid−liquid interfaces.

The outline of this paper is as follows. Section II briefly describes the polarizable model potentials and molecular dynamics simulation details utilized in this study. In section III, the simulation results describing the solvation structures, dynamics, and electrostatic properties of the K^+ ion in water, chloroform, and carbon tetrachloride are presented. In section IV, the solvation shell exchange kinetics is discussed and compared to the theoretical predictions. The conclusions are presented in section V.

TABLE 1: Potential Parameters for CCl_4, H_2O, $CHCl_3$, and K^+ Used in the MD Simulations[a]

molecule	atom type	σ (Å)	ϵ (kcal/mol)	q (e)	α (Å^3)
CCl_4	C	3.410	0.100	−0.1616	0.878
	Cl	3.450	0.260	0.0404	1.910
H_2O	H	0.000	0.000	0.3650	0.170
	O	3.205	0.160	−0.7300	0.528
$CHCl_3$	C	3.410	0.137	0.5609	0.878
	Cl	3.450	0.275	−0.1686	1.910
	H	2.810	0.020	−0.0551	0.135
K^+	K	3.154	0.100	1.0000	0.830

[a] σ and ϵ are the Lennard-Jones parameters, q is the atomic charge, and α is the atomic polarizability.

II. Potential Model and Computational Details

A. Potential Model. The molecular interactions of water, chloroform, carbon tetrachloride molecules, and K^+ ion are described with the use of polarizable potential models. The carbon tetrachloride−carbon tetrachloride,[13] water−water,[14] and chloroform−chloroform[15] potentials were developed previously in our laboratory to accurately reproduce thermodynamic, structural, and dynamical properties of water, carbon tetrachloride, and chloroform in various conditions. We realize that the ion dynamic may be distorted because the solvent molecules are kept rigid. A summary of the potential parameters employed in this study is listed in Table 1. The potassium ion is represented by a Lennard-Jones sphere with atomic charge and point polarizability. The potassium ion polarizability[16] is taken from the literature, and the Lennard-Jones parameters (σ and ϵ) are obtained by fitting to the experimental gas-phase incremental binding enthalpies[17] for the clusters $K^+-(H_2O)_n = 1-6$ as well as the hydration enthalpy[18] and structural properties[19] such as the radial distribution functions and the coordination number

10.1021/jp982079o CCC: $18.00
Published on Web 05/06/1999

TABLE 2: Properties of K^+ in Water at 300 K

(a) Computed and Experimental Cluster Binding Enthalpies of $K^+-(H_2O)_n$ at 300 K

n	MD	exptl[a]
1	-17.9 ± 0.1	-17.9
2	-34.1 ± 0.1	-34.0
3	-47.7 ± 0.2	-47.2
4	-58.8 ± 0.3	-59.0
5	-69.3 ± 0.4	-69.7
6	-78.5 ± 0.4	-79.7

(b) Structural and Thermodynamic Properties of K^+ in Water at 300 K

	MD	exptl
R_{IO} (Å)	2.75	2.79[b]
R_{IH} (Å)	3.35	
coordination no.	7.3	6.0, 7.0[b]
ΔH_{sol} (kcal/mol)	$-84. \pm 3$	-86[c]

[a] Reference 17. [b] Reference 19. [c] Reference 18.

for the ionic solution simulation as illustrated in Table 2. The potassium parameters are then used to model the K^+-CHCl_3 and K^+-CCl_4 interactions.

The total interaction energy of the system can be decomposed into pairwise additive and nonadditive components

$$U_{tot} = U_{pair} + U_{pol} \tag{1}$$

where the pair-additive part of the potential is simply a sum of the Lennard-Jones and Coulomb interactions,

$$U_{pair} = \sum_i \sum_j \left(4\epsilon \left[\left(\frac{\sigma_{ij}}{r_{ij}} \right)^{12} - \left(\frac{\sigma_{ij}}{r_{ij}} \right)^{6} \right] + \frac{q_i q_j}{r_{ij}} \right) \tag{2}$$

The nonadditive polarization energy is given by

$$U_{pol} = U_{stat} + U_{pp} + U_{self} \tag{3}$$

$$= -\sum_i \mu_i \cdot \mathbf{E}_i^0 - \frac{1}{2} \sum_j \sum_{j \neq i} \mu_i \cdot \mathbf{T}_{ij} \cdot \mu_j + \sum_i \frac{\mu_i \cdot \mu_i}{2\alpha_i} \tag{4}$$

Here, r_{ij} is the distance between site i and j, q is the charge, and σ and ϵ are the Lennard-Jones parameters. $\mathbf{E}_i^0$ is the electric field at site i produced by the fixed charges in the system, μ_i is the induced dipole moment at atom site i. $\mathbf{T}_{ij}$ is the dipole tensor. The first term in eq 4 represents the charge−dipole interaction, the second term describes the dipole−dipole interaction, and the last term is the energy associated with the generation of the dipole moment μ_i. During the molecular dynamics simulations, a standard iterative self-consistent field procedure is used to evaluate the induced dipoles.

In Figure 1, the gas-phase interaction potentials for the K^+-H_2O, K^+-CCl_4, and K^+-CHCl_3 dimers are shown as a function of the K^+-O or K^+-C distances along with the lowest-energy dimer structures. The optimal configuration of the K^+-H_2O complex is to have the O atom directly point toward the K^+ ion to maximize the electrostatic interaction. The minimum-energy structures of the K^+-CCl_4 and K^+-CHCl_3 dimers are very similar by having three chlorine atoms facing the K^+ ion with the fourth chlorine or hydrogen atom pointing away from K^+. The calculated binding energies are -18.2, -12.7, and -9.6 kcal/mol for the K^+-H_2O, K^+-CCl_4, and K^+-CHCl_3 dimers, respectively. As expected, the K^+ ion binds most strongly with H_2O. This effect is a direct consequence of the strong electrostatic interactions between K^+ and H_2O molecules. We

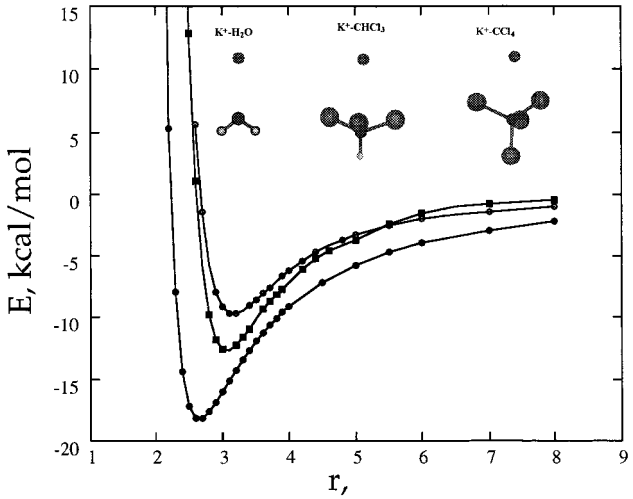

Figure 1. (a) Gas-phase intermolecular potential for K^+-H_2O (solid circles), K^+-CHCl_3 (open circles), and K^+-CCl_4 (squares) dimers as a function of the $K-O_{H_2O}$, $K-C_{CHCl_3}$, and $K-C_{CCl_4}$ distances, respectively. Insets are the lowest-energy structures of the K^+-H_2O, K^+-CHCl_3, and K^+-CCl_4 dimers.

observe that the K^+-CCl_4 dimer has a stronger binding energy than the K^+-CHCl_3 dimer despite the chloroform molecules possessing permanent dipole moments. This result can be resolved by examining the various binding energy components. It is found that the polarization contribution dominates the interaction energy at short K^+-C distances. Because CCl_4 has a larger molecular polarizability than $CHCl_3$, it is not surprising that the K^+-CCl_4 dimer binds more strongly than the K^+-CHCl_3 dimer. This also indicates that the molecular polarizability can play an important role in determining the ion−solvent interactions. As the K^+-C distance increases, the ion−dipole interaction becomes important and the K^+-CHCl_3 interaction becomes more energetically favorable than that of the K^+-CCl_4 dimer.

B. Computational Details. The molecular dynamics simulations are carried out on a system consisting of one potassium ion and 459 water, 265 carbon tetrachloride, or 265 chloroform molecules in a cubic simulation box with linear dimensions roughly of 24, 35, and 33 Å, respectively. Periodic boundary conditions are applied in all three spatial directions. The solvation properties of K^+ ion are obtained from simulations at a constant pressure of 1 atm and a temperature of 298 K (*NPT* ensemble) with the temperature and pressure coupling constants of 0.1 and 0.2 ps, respectively.[20] From a Maxwell−Boltzmann distribution corresponding to the desired simulation temperature, the initial velocity of each atom is randomly assigned. During the dynamics simulations, the SHAKE algorithm[21] is adapted to fix the internal molecular geometry by constraining all the bond lengths. The equations of motion are integrated using the leapfrog algorithm with a time step of 2 fs. The nonbonded interactions (i.e., Lennard-Jones, Coulombic, and polarization) are truncated at molecular center-of mass separations of 15, 15, and 9 Å for CCl_4, $CHCl_3$, and H_2O, respectively. This appoach has been shown to provide comparable results to the reaction field or Ewald summation techniques.[22] For this case, we strongly believe that this is a valid approach. The ion−solvent systems are equilibrated for 100 ps followed by a 200 ps molecular dynamics trajectory for data analysis.

III. Solvation Properties

In this section, solvation properties of K^+ ion in liquid H_2O, $CHCl_3$, and CCl_4 are discussed. Detailed solvation structures

are characterized by the atomic radial distribution functions. The electrostatic properties of the K^+ ion are examined via the induced dipole moment distributions. In addition, the dynamical behavior of the K^+ ion in H_2O, $CHCl_3$, and CCl_4 solutions is described in terms of velocity autocorrelation functions and residence time correlation functions.

A. Thermodynamics and Structural Properties. The K^+-H_2O, K^+-CHCl_3, and K^+-CCl_4 atomic pair correlation functions are depicted in parts a, b, and c of Figure 2, respectively. These radial distribution functions exhibit well-defined features, suggesting the existence of a local ion−solvent structural correlation. The sharp first peaks in these site−site distribution functions indicate that the solvent molecules form a tightly bound first coordination shell around the K^+ ion. The slightly higher first peak in the K^+-CCl_4 suggests that the K^+ ion induces more structuring in the first solvation shell of CCl_4 molecules relative to that of the bulk CCl_4 than in H_2O or $CHCl_3$. We also observe weak second peaks at larger ion−solvent distances, indicating loose second solvation shells. The running numbers of the solvent molecules in the first coordination shell of K^+ ion can be evaluated by integrating the ion−oxygen and ion−carbon radial distribution functions to their first minima. The results are listed in Table 3. The computed hydration number for K^+ in H_2O is 7.3, in good agreement with previous studies.[1,2] The coordination number of K^+ is found to be 8.0 in $CHCl_3$, which is slightly larger than that in H_2O. This result is attributed to the much larger coordination shell of $CHCl_3$ than that of H_2O, as clearly indicated by the peak positions in the radial distribution functions. Interestingly, although the first solvation shells for K^+ in CCl_4 and $CHCl_3$ are roughly the same size, the coordination number of CCl_4 is a much smaller value of 4.6. The difference comes from the fact that CCl_4 is considerably bigger than $CHCl_3$. Therefore, it is unfavorable to pack as many CCl_4 molecules around K^+ owing to the steric hindrance. In general, we found that the K^+ ion induces a strong molecular orientational correlation in liquid H_2O, $CHCl_3$, and CCl_4. However, this orientation order is only restricted to the neighboring solvent molecules. As the ion−solvent distance increases, the orientational order disappears.

B. Electrostatic Properties. In this section, the solvent effect on the induced dipole moment distributions of the K^+ ion and the orientation between the solvent dipole moment vectors and the K^+−solvent vector is investigated. Experiencing the electric field created by the surrounding solvent molecules, the K^+ ion becomes polarized and carries an induced dipole moment. The probability distributions of such induced dipole moments in liquid H_2O, $CHCl_3$, and CCl_4 are depicted in Figure 3. It is found that the induced dipole moments of K^+ become broader and shift to a larger average value from chloroform to carbon tetrachloride to water. Clearly, because of the large permanent dipole moments of the water molecules, water induces a strong local electric field around the K^+ cation, which leads to large dipole moments of K^+. Interestingly, the average induced dipole moment of K^+ is smaller in liquid $CHCl_3$ than that in CCl_4, despite the fact that $CHCl_3$ possesses permanent dipole moments while CCl_4 is a nonpolar liquid. This result may be explained partly in terms of the greater molecular polarizability of CCl_4 and partly in terms of more pronounced molecular orientational correlation between the K^+ cation and the CCl_4 molecules. Because CCl_4 is highly polarizable, the presence of the K^+ ion induces large dipole moments of the CCl_4 molecules. This, together with the strong K^+-CCl_4 orientational order, causes the large average induced dipole moment of the K^+ ion.

C. Dynamical Properties. The dynamical properties of the

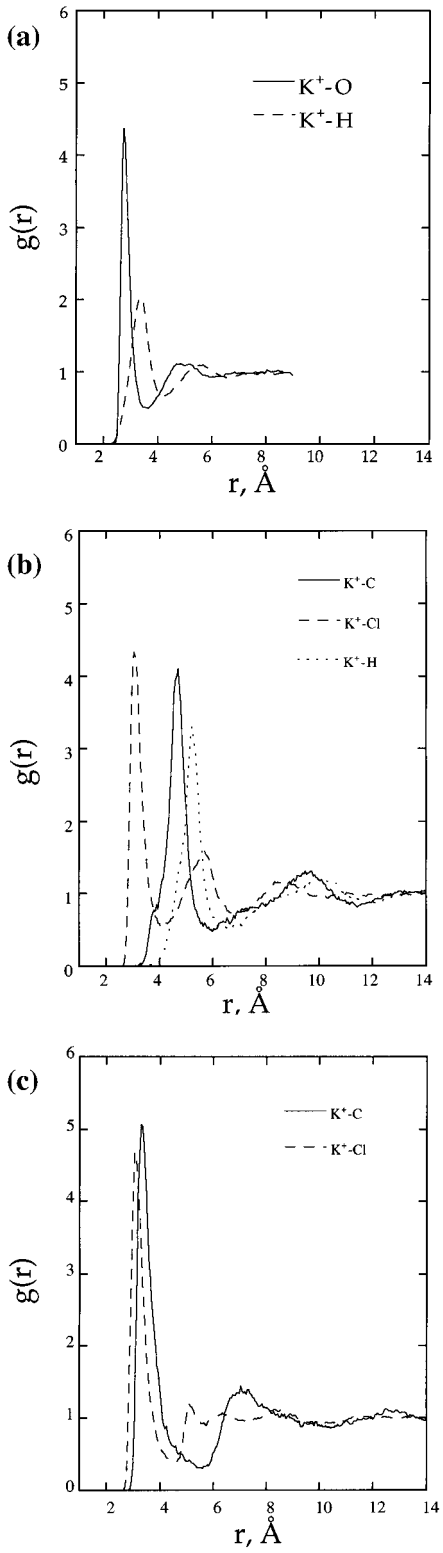

Figure 2. Computed atomic radial distribution functions for (a) K^+-O (circles) and K^+-H (squares) in liquid water, (b) K^+-C (squares), K^+-Cl (circles), and K^+-H (diamonds) in liquid chloroform, and (c) K^+-C (circles) and K^+-Cl (squares) in liquid carbon tetrachloride at 298 K.

K^+ ion and the solvent molecules are examined via velocity autocorrelation functions, mean-square displacements, and residence time correlation functions. These analyses not only yield macroscopic information such as self-diffusion coefficients but also provide a microscopic description of the relative motion between the K^+ ion and the solvent molecules.

To gain molecular insight into the dynamical behavior of K^+,

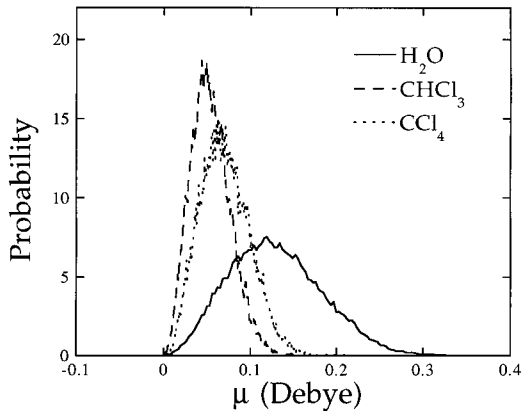

Figure 3. Computed induced dipole moment distributions of K^+ ion in (a) H_2O (solid lines), (b) $CHCl_3$ (dashed lines), and (c) CCl_4 (dotted lines) at 298 K.

TABLE 3: Dimer Energy, Average Coordination Number, Diffusion Coefficients (Calculated from the Velocity Autocorrelation Functions (VACF) and the Mean-Square Displacement (MSD)), and the Residence Time for the K^+ Ion in Liquid Water, Chloroform, and Carbon Tetrachloride at 298 K

property	K^+ in H_2O	K^+ in $CHCl_3$	K^+ in CCl_4
dimer energy (kcal/mol)	−18.3	−9.7	−12.7
coordination number	7.3	8.0	4.6
D (10^{-5} cm^2/s) (MSD)	3.7 ± 0.2	2.1 ± 0.1	2.2 ± 0.1
D (10^{-5} cm^2/s) (VACF)	3.7 ± 0.2	2.0 ± 0.1	1.8 ± 0.1
residence time (ps)	9.4	30.8	29.6

we compute the normalized velocity autocorrelation functions, which is defined as[23]

$$C_{VV}(t) = \frac{\langle \vec{V}(0)\cdot\vec{V}(\tau)\rangle}{\langle \vec{V}(0)\cdot\vec{V}(0)\rangle} \quad (5)$$

where $V(\tau)$ is the velocity of the ion at time τ and $\langle ...\rangle$ denotes an ensemble average. In parts a, b, and c of Figure 4, the normalized velocity autocorrelation functions are shown for K^+ in liquid water, chloroform, and carbon tetrachloride as a function of time, respectively. Interestingly, the overall features of the ion velocity autocorrelation functions are fairly similar in $CHCl_3$ and CCl_4 but show noticeable discrepancy in liquid H_2O. This implies that the motion of the K^+ ion in the aqueous phase behaves differently than that in liquid $CHCl_3$ and CCl_4. Clearly, all the velocity autocorrelation functions show a rapid initial decay to zero in about 0.4 ps. The distinct features of the K^+ velocity autocorrelation function in H_2O depicted in Figure 4a suggest that there is more than one frequency contributing to the correlation function. On the other hand, the velocity autocorrelation functions of the K^+ ion in liquid chloroform and carbon tetrachloride appear to follow a damped oscillation, which can be characterized by one single frequency. The oscillatory behavior of $C_{VV}(t)$ in liquid $CHCl_3$ and CCl_4 at short times possibly comes from the rattling motion of the K^+ ion inside the first solvation cage formed by these solvent molecules. From the velocity autocorrelation function, the diffusion coefficient can be determined on the basis of the Green−Kubo relation[24]

$$D = \frac{1}{3}\lim_{t\to\infty}\int_0^t \langle \vec{V}(0)\cdot\vec{V}(\tau)\rangle \, d\tau \quad (6)$$

The computed diffusion constants from the velocity autocorrelation functions are summarized in Table 3. We found that the K^+ ion diffuses much more rapidly in H_2O than in $CHCl_3$ and CCl_4. This result is consistent with the residence time of the first solvation shell solvent molecules, as will be discussed in a later section. From molecular dynamics simulations, the self-diffusion coefficients of the K^+ ion in the bulk liquid can also be evaluated conveniently from the mean-square displacement based on a well-known relation

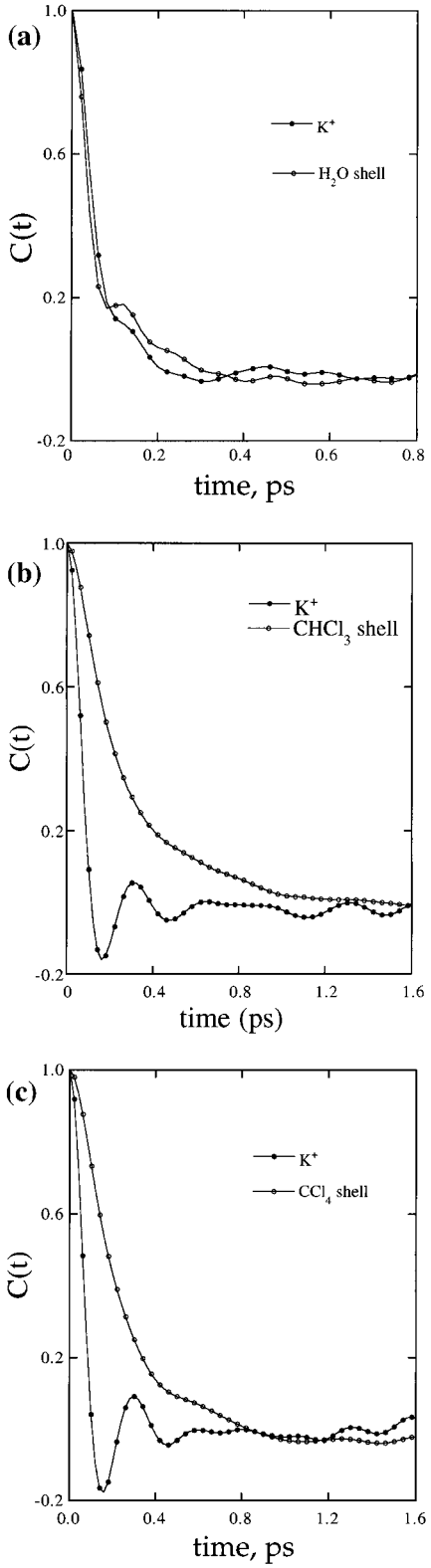

Figure 4. Normalized velocity autocorrelation functions $C_{VV}(t)$ of the K^+ ion (circles) and its first solvation shell $C_{ss}(t)$ (open circles) for K^+ in (a) water, (b) chloroform, and (c) carbon tetrachloride.

$$D = \frac{1}{6}\lim_{t\to\infty}\frac{\mathrm{d}}{\mathrm{d}t}\langle|\vec{r}(t) - \vec{r}(0)|^2\rangle \quad (7)$$

where $r(t)$ is the coordinate of the K^+ ion at time t. The computed ion mean-square displacements are displayed in Figure 5 as a function of time for K^+ in liquid H_2O, $CHCl_3$, and CCl_4, respectively. The diffusion coefficients are determined from the least-squares fits to the mean-square displacements and are listed in Table 3. It is clear that the diffusion coefficients estimated from the mean-square displacements and ion velocity autocorrelation functions are in reasonable agreement with each other. The diffusion coefficient of K^+ in liquid H_2O is compared well with other theoretical data such as that of ref 3b, but they overestimated the experimental value.

To further examine the dynamical properties of the solvent molecules around the K^+ cation, we evaluate the center-of-mass velocity autocorrelation functions of the first solvation shell. Let $V_s(t)$ be the sum of the center-of-mass velocity of the solvent molecules that form the first coordination shell around K^+, the velocity autocorrelation function of the solvation shell, $C_{ss}(t)$, can be defined as[1]

$$C_{ss}(t) = \frac{\langle\vec{V}_s(0)\cdot\vec{V}_s(t)\rangle}{\langle\vec{V}_s(0)\cdot\vec{V}_s(0)\rangle} \quad (8)$$

Here, the radius of the first solvation shell is defined by the positions of the first minima in the ion−solvent pair correlation functions. The resulting first solvation shell velocity autocorrelation functions as a function of time are depicted in parts a, b, and c of Figure 4 for K^+ bulk H_2O, $CHCl_3$, and CCl_4, respectively. Again, we note that the velocity autocorrelation functions of the first solvation shells behave very similarly for K^+ in liquid $CHCl_3$ and CCl_4 but are noticeably different from the correlation function for K^+ in H_2O. Interestingly, the $C_{VV}(t)$ and $C_{ss}(t)$ for the K^+ ion in liquid H_2O decay on the same time scale and exhibit significant similarity with each other. A similar behavior has been observed in previous studies and implies that the K^+ ion moves in a quasi-continuum.[1] It has also been suggested that the oscillatory component of the water hydration shell velocity correlation functions comes from the coupling of the motion between the water molecules in the first solvation shell and those in the bulk. The velocity autocorrelation functions of the first coordination shells for K^+ in liquid $CHCl_3$ and CCl_4 appear to follow an exponential decay with a time scale that is longer than the corresponding ion velocity autocorrelation functions. These results may indicate that the motion of the $CHCl_3$ and CCl_4 molecules in the first solvation shell around the K^+ ion is not affected by the presence of the K^+ ion. The difference in the $C_{ss}(t)$ of liquid H_2O compared to those of liquid $CHCl_3$ and CCl_4 may be due to the fact that H_2O molecules interact with each other with strong directional bonding, while $CHCl_3$ and CCl_4 have rather weak isotropic intermolecular interactions.

By analysis of the residence time correlation function of the first solvation shell solvent molecules, more insight can be gained into the relative motion between the K^+ ion and the solvent molecules. The residence time correlation function yields an estimate of the time scale for a solvent molecule in the first coordination shell and is defined as[3,4]

$$R(r,t) = \frac{1}{N_r}\sum_{i=1}^{N_r}[\theta(r,0)\theta(r,t)] \quad (9)$$

Here, $\theta(r,t)$ is the Heavyside step function, which equals 1 if the solvent molecule i stays inside the first coordination shell and 0 when the solvent molecule leaves the first solvation shell. N_r is simply the average number of the solvent molecules in the first coordination shell (coordination number), and t is the time. The residence correlation functions as a function of time are displayed in Figure 6 for the K^+ ion in liquid H_2O, $CHCl_3$, and CCl_4. Clearly, these correlation functions can be reasonably described by an exponential decay. The residence time of the solvent molecules in the first solvation shell is obtained by fitting the correlation functions to an exponential decay function and is summarized in Table 3. The computed residence time of water molecules agrees reasonably well with other theoretical data such as that of ref 1 (i.e., 9.4 versus 4.8 ps).

In Figure 6, it is obvious that the residence time correlation functions for liquid $CHCl_3$ and CCl_4 are nearly on top of each other and decay more slowly than that for water molecules. The computed residence times of the $CHCl_3$ and CCl_4 molecules are more than 3 times of that of the H_2O molecules. This trend at first seems to contradict our expectation based on an energetic consideration: the ion−water interaction is much stronger than the ion−CCl_4 and ion−$CHCl_3$ interactions. Thus, it is anticipated that the residence time of H_2O should be longer than that of $CHCl_3$ and CCl_4. However, it should be realized that other

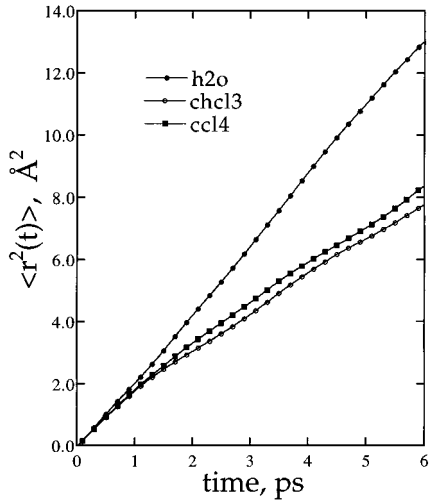

Figure 5. Mean-square displacements of the K^+ ion in water (solid circles), $CHCl_3$ (open circles), and CCl_4 (diamonds) from MD simulations at 298 K.

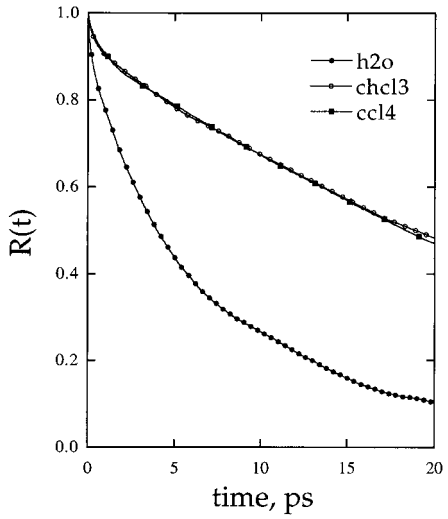

Figure 6. Residence time autocorrelation function for the first solvation shell solvent molecules around the K^+ ion in water (solid circles), $CHCl_3$ (open circles), and CCl_4 (diamonds).

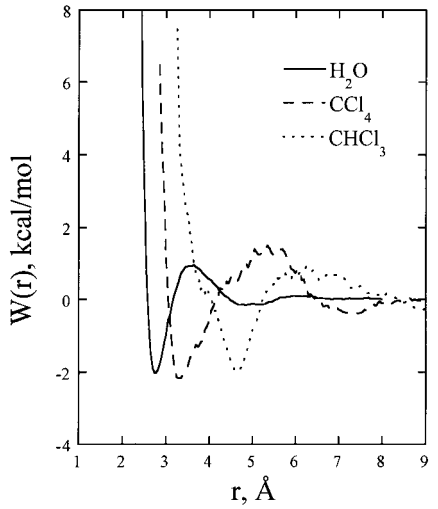

Figure 7. Computed potential of mean force: (a) K^+-O in water (solid); (b) K^+-C in liquid carbon tetrachloride (dashed); (c) K^+-C in liquid chloroform (dotted).

interaction energy scales need to be considered. For example, the H_2O-H_2O bonding is much stronger than the CCl_4-CCl_4 and $CHCl_3-CHCl_3$ interactions. It is plausible that the strong coupling of the motion between the H_2O molecules in the first and the second solvation shell is responsible for the fast decay rate of the residence time autocorrelation function for K^+ in liquid H_2O. It has also been suggested that the breakup of the first solvation shell is caused by the molecular reorientation.[1] Therefore, it will be more difficult for large molecules such as chloroform and carbon tetrachloride to reorient owing to the steric hindrance, which leads to a longer residence time.

IV. Solvation Shell Exchange Process

The exchange of the solvent molecule in the first solvation shell of an ion is of fundamental importance to the ion transport processes and ion reactions in bulk liquid. In this section, the dynamical reaction rates of the solvation shell exchange processes will be investigated with the constrained molecular dynamics simulation techniques similar to those employed in the ion association processes in the liquid phase.

The reaction rate of an ion−solvent dissociation reaction, k, can be written as

$$k = \kappa k^{\mathrm{TST}} \tag{10}$$

Here, k^{TST} is the rate constant predicted by the classical transition-state theory. κ is the transmission coefficient that takes into account the dynamical corrections such as recrossing and tunneling effects. By modeling the solvent exchange process as a unimolecular dissociation reaction, we can define the reaction coordinate as the distance between the K^+ cation and the center of mass of the solvent molecule.[25] The potential of mean force, $w(r)$, governing this dissociation process can simply be expressed as

$$W(r) = -\beta^{-1} \ln(g(r)) \tag{11}$$

where $\beta = (k_b T)^{-1}$, k_b is the Boltzmann constant, and $g(r)$ is the radial distribution function between the ion and the solvent molecule. These computed potentials of mean force are given in Figure 7. From the potential of mean force, the reaction rate predicted by assuming equilibrium solvation and transition-state theory is then[26,27]

$$k^{\mathrm{TST}} = \sqrt{\frac{k_b T}{2\pi\mu}} \frac{r^{\ddagger 2}\, e^{-\beta w(r^{\ddagger})}}{\int_0^{r^{\ddagger}} dr\, r^2\, e^{-\beta w(r)}} \tag{12}$$

where μ is the ion−solvent molecule pair reduced mass. $r^{\ddagger}$ is the position of the barrier top of the mean-force potential. The computed rate constants from the classical transition-state theory for K^+-solvent dissociation reaction in liquid H_2O, $CHCl_3$, and CCl_4 are summarized in Table 4. These results may be compared directly with the inverse of the residence times of the solvent molecules in the first solvation shell, which are 0.106, 0.032, and 0.034 ps^{-1} for K^+ in H_2O, $CHCl_3$, and CCl_4, respectively. It is clear that the classical transition-state theory significantly overestimates the dissociation rate. This is due to the fact that the transition-state theory neglects the dynamical coupling between the solute and the solvent molecules at the barrier top region.

TABLE 4: Rate Theory Results for K^+ in H_2O, $CHCl_3$, and CCl_4

	H_2O	$CHCl_3$	CCl_4
k^{TST} (ps^{-1})	0.76	0.29	0.21
ω_b (ps^{-1})	13.8	2.9	6.4
κ_{GH}	0.28	0.10	0.24
$k = \kappa_{GH} k^{\mathrm{TST}}$ (ps^{-1})	0.21	0.03	0.05
1/residence time (ps)	0.11	0.03	0.03

One theoretical treatment that attempts to include such dynamical effects is the Grote−Hynes theory,[28] which is based on the generalized Langevin equation approach and is shown to be successful in the applications to many chemical reactions. In the Grote−Hynes theory, the transmission coefficient, k_{GH}, is given by

$$\kappa_{GH} = [\kappa_{GH} + (1/\omega_b)\int_0^{\infty} e^{-\omega_b \kappa^{GH} t} \zeta(t)\, dt]^{-1} \tag{13}$$

where $\zeta(t)$ is the time-dependent friction kernel acting on the reaction coordinate and ω_b is the barrier frequency at the transition state, which is obtained by fitting the maximal region of the potential of mean force to an inverted parabola. The computed values of ω_b from the mean-force potential are listed in Table 4. The barrier frequency is highest in H_2O, then decreases from CCl_4 to $CHCl_3$. It should be noted that a large uncertainty is found to be associated with the low barrier frequency, which will affect the computed transmission coefficient.

On the basis of the fluctuation−dissipation theorem, the reaction coordinate friction function, $\zeta(t)$, is related to the fluctuations of the force exerted on the reaction coordinate axis, $\delta F(r,t)$,[29]

$$\zeta(t;r) \equiv (\beta/\mu)\langle \delta F(t;r) \delta F(0;r) \rangle \tag{14}$$

Here, r is the distance between the K^+ ion and the center of mass of the solvent molecule. In the Grote−Hynes treatment, r is fixed at the barrier top position. To investigate the solvation shell exchange process, a second set of molecular dynamics simulations is performed in a canonical ensemble (*NVT*) with periodic boundary conditions applied in all three directions. The statistical analysis is performed from data collected over a 300 ps period, following a 100 ps simulation of equilibration. The fluctuations of the force exerted on the reaction coordinate for various solvents are summarized in Figure 8.

The resulting transmission coefficients and the dissociation rate constants are displayed in Table 4. Compared to the classical

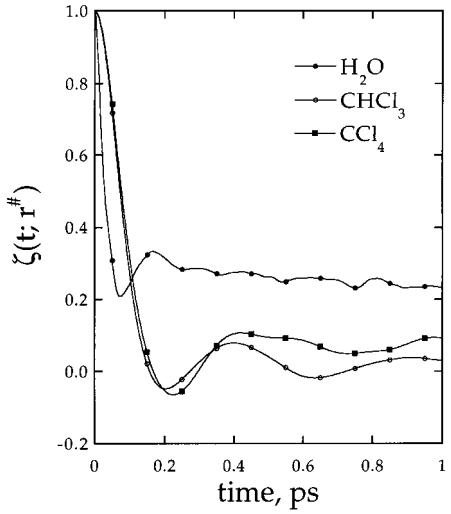

Figure 8. Fluctuation of the force exerted on the reaction coordinate for the K^+ ion in H_2O (solid circles), $CHCl_3$ (open circles), and CCl_4 (diamonds).

transition-state theory, the inclusion of the Grote−Hynes corrections gives much better estimates of the dissociation rates. The discrepancy between the Grote−Hynes predictions and the inverse of the residence times may be due to the neglect of the effects of the anharmonicity and the distance-dependent friction functions. More refined theories may be needed to get a more accurate estimate of the rate constant.[30] It should also be noted that the transmission coefficients are fairly sensitive to the barrier frequency and the details of the mean-force potential, and the rate constants may be changed by 40% from the uncertainty in the barrier frequency.

V. Conclusions

Using classical molecular dynamics simulation techniques, we have examined the solvation properties and the ion-solvation shell exchange processes of a K^+ ion in liquid H_2O, $CHCl_3$, and CCl_4. In these studies, the ion−solvent and solvent−solvent interactions are described using many-body polarizable potential models.

The sharp features in the atomic radial distribution functions reveal that H_2O, $CHCl_3$, and CCl_4 molecules form well-defined solvation shells around the K^+ ion. The coordination numbers are 7.3, 8.0, 4.6 in liquid H_2O, $CHCl_3$, and CCl_4, respectively. This result is well understood in terms of the size of the solvation shells and the solvent molecules.

It is found that the induced dipole moments of K^+ become broader and shift to a larger average value from chloroform to carbon tetrachloride to water. This trend can be explained in terms of the molecular polarizabilities and the permanent dipole moments of the solvent molecules.

We have estimated the diffusion coefficients of K^+ in liquid H_2O, $CHCl_3$, and CCl_4 from both the mean-square displacements and the velocity autocorrelation functions. In general, the computed diffusion constants are in good agreement with each other. The K^+ ion is found to diffuse more rapidly in the aqueous phase, compared to that in liquid $CHCl_3$ and CCl_4. More insight to the dynamics properties of the ion−solvent systems was gained by examining the velocity autocorrelation functions of the first solvation shell of the H_2O, $CHCl_3$, and CCl_4 molecules. We found that the autocorrelation functions of the organic solvents behave fairly similarly but are very different from that of H_2O. By inspection of the residence time autocorrelation functions, an estimate of the time period that a solvent molecule remains in the first coordination shell can be obtained. The residence time of H_2O is found to be 9.4 ps, which is considerably shorter than the 30 ps time scale of the $CHCl_3$ and CCl_4 molecules.

The solvation shell exchange process is also examined with the molecular dynamics simulations. The mean-force potentials governing this process is obtained from the ion−solvent molecule pair correlation functions. It is found that an estimate using equilibrium solvation and classical transition-state theory consistently overestimates the dissociation rate of the K^+ ion and the solvent molecule. Including the dynamical effects in an approximate manner such as Grote−Hynes theory yields more accurate dissociation rates.

Acknowledgment. This work was performed under the auspices of the Division of Chemical Sciences, Office of Basic Energy Sciences, U.S. Department of Energy under Contract DE-AC06-76RLO 1830 with Battelle Memorial Institute, which operates the Pacific Northwest National Laboratory, a multi-program national laboratory. Computer resources were provided by the Division of Chemical Sciences and by the Scientific Computing staff, Office of Energy Research, at the National Energy Research Supercomputer Center (Berkeley, CA).

References and Notes

(1) Impey, R. W.; Madden, P. A.; McDonald, I. R. *J. Phys. Chem.* **1983**, *87*, 5071.
(2) Nguyen, H. L.; Adelman, S. A. *J. Chem. Phys.* **1984**, *81*, 4564.
(3) Lee, S. H.; Rasaiah, J. C. *J. Chem. Phys.* **1994**, *101*, 6964. Lee, S. H.; Rasaiah, J. C. *J. Phys. Chem.* **1996**, *100*, 1420.
(4) Cannon, W. R.; Pettitt, B. M.; McCammon, J. A. *J. Phys. Chem.* **1994**, *98*, 6225.
(5) Hynn, J. K.; Ichiye, T. *J. Phys. Chem. B* **1997**, *101*, 3596.
(6) Mezei, M.; Beveridge, D. L. *J. Chem. Phys.* **1981**, *74*, 6902.
(7) Smith, D. E.; Dang, L. X. *J. Chem. Phys.* **1994**, *100*, 3757.
(8) Chandrasekhar, J.; Jorgensen, W. L. *J. Chem. Phys.* **1982**, *77*, 5080.
(9) Chandrasekhar, J.; Jorgensen, W. L.; Bigot, B. *J. Am. Chem. Soc.* **1982**, *104*, 4584. Sese, G.; Guardia, E. *J. Phys. Chem.* **1995**, *99*, 12647. Madhusoodanan, M.; Tembe, B. L. *J. Phys. Chem.* **1995**, *99*, 44.
(10) Impey, R. W.; Sprik, M.; Klein, M. L. *J. Am. Chem. Soc.* **1987**, *109*, 5900. Rao, B. G.; Singh, U. C. *J. Am. Chem. Soc.* **1990**, *112*, 3803.
(11) Haag, W. R.; Yao, C. C. D. *Environ. Sci. Technol.* **1992**, *26*, 1005. U.S. Department of Energy, Office of Environmental Management, FY 1995 Technology Development Needs Summary, 1994; pp 2−17.
(12) Koeing, K. E.; Lein, G. M.; Stucker, P.; Kaneda, T.; Cram, D. *J. Am. Chem. Soc.* **1979**, *101*, 3553.
(13) Chang, T.-M.; Dang, L. X.; Peterson, K. A. *J. Chem. Phys.* **1997**, *101*, 3413.
(14) Dang, L. X. *J. Chem. Phys.* **1992**, *97*, 2659.
(15) Chang, T.-M.; Dang, L. X.; Peterson, K. A. *J. Phys. Chem. B* **1997**, *101*, 3413.
(16) Pauling, L. *Proc. R. Soc. London* **1927**, *A114*, 181.
(17) Arshadi, M.; Yamdagni, R.; Kebarle, P. *J. Phys. Chem.* **1970**, *74*, 1475.
(18) Friedman, H. L.; Krischnan, C. V. In *Water: A Comprehensive Treatise*; Franks, F., Ed.; Plenum: New York, 1973; Vol. 6, p 1.
(19) Marcus, Y. *Chem. Rev.* **1988**, *88*, 1475−1498 and references therein.
(20) Berendsen, H. J. C.; Postma, J. P.; Di Nola, A.; Van Gunsteren, W. F.; Haak, J. R. *J. Chem. Phys.* **1984**, *81*, 3684.
(21) Ryckaert, J.; Ciccotti, G.; Berendsen, H. J. C. *J. Comput. Phys.* **1977**, *23*, 327.
(22) Perera, L.; Essmann, U.; Berkowitz, M. *J. Chem. Phys.* **1995**, *102*, 450.
(23) Bopp, P. In *The Physics and Chemistry of Aqueous Ionic Solutions*; Bellissent-Funel, M. C., Neilson, G. W., Eds.; D. Reidel Publishing: Dordrecht, 1987; p 217.
(24) McQuarrie, D. A. *Statistical Mechanics*; Harper and Row: New York, 1976.
(25) Rey, R.; Hynes, J. T. *J. Phys. Chem.* **1996**, *100*, 5611.
(26) Ciccotti, G.; Farrario, M.; Hynes, J. T.; Kapral, R. *Chem. Phys.* **1989**, *129*, 241.
(27) Ciccotti, G.; Farrario, M.; Hynes, J. T.; Kapral, R. *J. Chem. Phys.* **1990**, *93*, 713.
(28) Rey, R.; Guàrdia, E.; Padró, J. A. *J. Chem. Phys.* **1992**, *97*, 1343.
(29) Hynes, J. T. In *The Theory of Chemical Reaction Dynamics*; Baer, M., Ed.; CRC: Boca Raton, FL, 1985; Vol. 55, p 549.
(30) Voth, G. A. *J. Chem. Phys.* **1992**, *97*, 5908.